States in ^{126}Sb populated in the β decay of 10^5-yr ^{126}Sn†

H. A. Smith, Jr.,* M. E. Bunker, J. W. Starner, and C. J. Orth
University of California, Los Alamos Scientific Laboratory, Los Alamos, New Mexico 87544

K. E. G. Löbner
Technical University, Munich, Germany
and University of California, Los Alamos Scientific Laboratory, Los Alamos, New Mexico 87544

(Received 8 September 1975)

The low-energy level structure of the odd-odd nucleus ^{126}Sb has been investigated by studying the radioactive decay of 10^5-yr ^{126}Sn, using Ge(Li) and Si(Li) detectors. Based on conversion-electron and γ-ray singles data, γ-γ and γ-e^- prompt and delayed coincidence measurements, and complementary γ-ray energy and intensity balance arguments, a decay scheme for ^{126}Sn has been deduced which accommodates all of the observed γ-ray transitions. The energies (keV), spins, and parities of the levels established in ^{126}Sb are as follows: 0.0 [8$^-$], 17.7 [5$^+$], 40.4 [3$^-$], 83.1 [4$^-$, (3$^-$)], 104.7 [3$^+$], and 128.0 [2$^+$]. The respective half-lives of these six states are: 12.4 day, 19.0 min, ≈11 s, 5.1 ns, 553 ns, and 78.0 ns, the latter four values having been determined in the present investigation. The level assignments are discussed within the framework of the single-particle shell model and in relation to the proposed assignments of low-lying energy levels of neighboring odd-odd antimony isotopes.

[RADIOACTIVITY ^{126}Sn [from ^{235}U(n,f)]; measured E_γ, I_γ, I_{ce}, γ-γ, β-γ, and e-γ coin, level $T_{1/2}$'s; deduced ICC, γ multipolarities, ^{126}Sb levels, J, π; calculated γ-hindrance factors. Ge(Li), Si(Li) detectors; mass-separated source.]

I. INTRODUCTION

The low-lying level spectra of several of the odd-odd antimony isotopes have been the subject of numerous experimental investigations. Theoretical studies of these results and of the level spectra of other odd-odd nuclei in the so-called "vibrational" region have been attempted with the particular objective of learning more about the effective neutron-proton force.[1-5] In the simplest version of the shell model, in which all residual interactions are ignored, the states in a multiplet arising from a given proton and neutron configuration are degenerate in energy. However, an effect of both the long-range collective interactions and the short-range neutron-proton interaction is to break this degeneracy, and it is therefore important to establish the systematic trends in the energy ordering of the lowest levels in these nuclei in order that various theoretical formulations of the residual-force interactions can be tested against experiment.

The present work describes an investigation of the low-lying (< 130 keV) energy levels in ^{126}Sb which are populated in the β decay of the ^{126}Sn ground state. In the most recent study of the ^{126}Sn decay,[6] evidence for five excited states below approximately 130 keV was obtained, and the lifetimes of two of these levels were determined. Also, possible spin and parity assignments for the observed levels were discussed. No level energies, however, were determined because the 19-min isomeric transition from the first excited state to the ground state of ^{126}Sb was unobserved. Also, the order of the (21-42)-keV γ-γ cascade was not established. In the present work γ-ray transitions, conversion lines, and level lifetimes, in addition to those measured in Ref. 6, are reported. From these data, an essentially complete decay scheme for ^{126}Sn has been deduced. Also, firm spin and parity assignments have been made for all six of the observed ^{126}Sb levels, significantly extending the systematics of the low-lying energy levels of the odd-odd antimony ($Z = 51$) nuclei.

II. EXPERIMENTAL PROCEDURE

A. Source preparation

The ^{126}Sn source used in most of the measurements described here was deposited on 0.005 cm aluminum foil in the Aldermaston isotope separator.[7] Further details of the preparation of the source material are given in Ref. 6. The source strength was about 500 dis/s.

B. Singles γ spectrum

The singles γ-ray spectrum emitted by the ^{126}Sn source was measured with an Ortec photon spectrometer, which incorporated a small Ge(Li) detector with resolution full width at half maximum

(FWHM) approximately equal to 200 eV at 6 keV. The results of this measurement are displayed in Fig. 1 and are summarized numerically in Table I.

Two new transitions were observed in this measurement, namely, those of energy 86.9 and 22.7 keV. A number of other lines below 20 keV were also observed, but all of these were identified as Sb and Te L x rays, fluorescence lines from gold, germanium, and nickel, or germanium $K\alpha$ and $K\beta$ escape peaks. In a singles γ-ray spectrum measurement with a lithium-drifted silicon detector (and similar resolution), all of these peaks except those due to Sb and Te L x rays were absent, indicating that the missing peaks were in fact associated with the Ge(Li) detector system.

C. β-γ coincidence measurements

Two of the levels in ^{126}Sb were previously known to be isomeric, with respective half-lives of 19 min and 0.5 μs.[6] Based upon the most recent de-

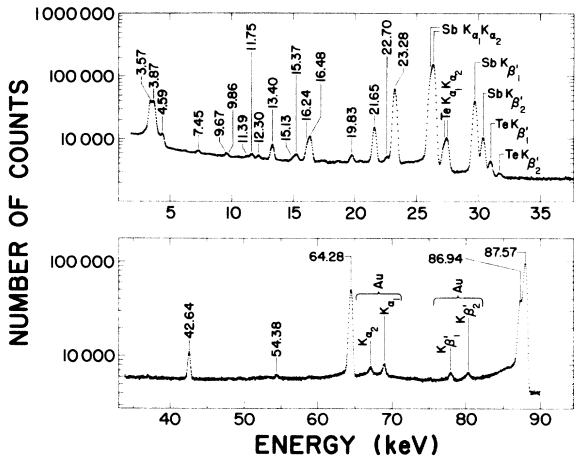

FIG. 1. The γ-ray singles spectrum from the decay of ^{126}Sb, taken with a Ge (Li) photon spectrometer (resolution approximately 200 eV at 6 keV. The peaks are labeled according to their energy (keV) except for the x rays, which are denoted by their origin.

TABLE I. Analysis of Ge(Li) photon spectrometer data of Fig. 1.

Line energy (keV)	Relative intensity [a]	Remarks
3.571 ± 0.010	14.85	Sb, Te L x rays
3.868 ± 0.010	14.44	
4.594 ± 0.010	0.81	
7.452 ± 0.020	0.22	Ni $K\alpha_1$, $K\alpha_2$
9.671 ± 0.030	0.14	Au $L\alpha_1$
9.856 ± 0.050	0.07	Ge $K\alpha_1$, $K\alpha_2$
11.387 ± 0.035	0.10	Au $L\beta_1$
11.749 ± 0.015	0.29	$K\alpha$(Ge) escape peak of 21.646
12.295 ± 0.020	0.20	$K\beta$(Ge) escape peak of 23.280
13.400 ± 0.010	1.21	$K\alpha$(Ge) escape peak of 23.280
15.132 ± 0.025	0.19	$K\beta$(Ge) escape peak of Sb $K\alpha_2$
15.374 ± 0.015	0.34	$K\beta$(Ge) escape peak of Sb $K\alpha_1$
16.236 ± 0.013	1.14	$K\alpha$(Ge) escape peak of Sb $K\alpha_2$
16.484 ± 0.010	1.97	$K\alpha$(Ge) escape peak of Sb $K\alpha_1$
19.833 ± 0.014	0.39	$K\alpha$(Ge) escape peak of Sb $K\beta'_1$
21.646 ± 0.010	3.35	
22.702 ± 0.067	0.27	
23.280 ± 0.010	17.3	
26.107 ± 0.010	21.42	Sb $K\alpha_2$
26.358 ± 0.010	40.44	Sb $K\alpha_1$
27.227 ± 0.010	1.09	Te $K\alpha_2$
27.484 ± 0.010	1.88	Te $K\alpha_1$
29.715 ± 0.003	11.6	Sb $K\beta'_1$
30.386 ± 0.010	2.38	Sb $K\beta'_2$
30.985 ± 0.010	0.56	Te $K\beta'_1$
31.711 ± 0.030	0.12	Te $K\beta'_2$
42.641 ± 0.010	1.35	
54.376 ± 0.030	0.12	$K\alpha$(Ge) escape peak of 64.281
64.281 ± 0.010	25.9	
66.986 ± 0.020	0.37	Au $K\alpha_2$
68.801 ± 0.005	0.59	Au $K\alpha_1$
77.735 ± 0.020	0.34	Au $K\beta_1$
79.436 ± 0.030	0.15	Au $K\beta_2$
86.938 ± 0.010	24.1	
87.567 ± 0.010	100.0	

[a] Uncertainties in these values are ±10% for intensities >0.5.

cay scheme[6] and the systematics of $E1$ transition lifetimes,[8] it also appeared likely that the level in ^{126}Sb to which most of the β decay proceeds ($E \approx 0.13$ MeV) should have a lifetime measurable via delayed-coincidence counting.

The half-life of the level near 0.13-MeV was measured by the conventional delayed-coincidence method, with an Ortec time-to-amplitude converter (TAC) in the fast part. The TAC was started by β particles detected in a plastic scintillator and was stopped by γ rays detected in a NaI(Tl) crystal. The two single-channel analyzers of the slow coincidence circuit selected, respectively, β particles with energy below 250 keV and γ rays between 55 and 95 keV (which includes the 64.3-, 86.9-, and 87.6-keV transitions). The measured time spectrum showed, on the right-hand side of the time distribution (corresponding to delay of the γ rays), slopes corresponding to half-lives of 78.0 ± 0.5 and 553 ± 5 ns. A plot of this TAC spectrum is shown in Fig. 2. The counts in the prompt spike are mainly attributable to β-γ coincidences associated with the decay of ^{126}Sb to the levels in ^{126}Te.

In order to determine which γ rays are associated with the above two half-lives, a second delayed β-γ coincidence measurement was performed. For this measurement the NaI(Tl) detector was replaced with the photon spectrometer, and the γ-ray spectrum in coincidence with pulses in selected time regions of the TAC output spectrum were recorded with a multichannel analyzer. γ spectra delayed $\lesssim 150$ and $\gtrsim 500$ ns were recorded. The results obtained indicate that the 78-ns level in ^{126}Sb is depopulated by 87.6- and 23.3-keV γ-ray transitions, and the 500-ns level is depopulated by 86.9-, 64.3-, and possibly the 42.6-keV γ transitions.

D. γ-γ coincidence measurements

To obtain further information about the placement of certain γ rays, a series of γ-γ coincidence measurements was performed. In the first of these, a single-channel analyzer selected the 23.3-keV γ ray (detected with the photon spectrometer), and a 60-cm^3 Ge(Li) detector viewed the ^{126}Sn γ-ray spectrum in the energy range 10 to 100 keV. The two outputs were fed into a slow coincidence circuit (coincidence resolving time equal to 4 μs). The spectrum of γ rays detected in the 60-cm^3 Ge(Li) detector which were in coincidence with the 23.3-keV γ ray was stored in a multichannel analyzer. The resulting coincidence spectrum showed 64- and 87-keV peaks with about equal intensity, consistent with the placement of the 64.3- and 86.9-keV transitions in the proposed decay scheme (Fig. 6).

In order to establish the order of emission of the two γ rays (21.7 and 42.6 keV) that cascade through the proposed third excited state, a γ-γ delayed coincidence measurement involving these two transitions was undertaken. In view of the low source strength and the fact that both the 21.7- and the 42.6-keV transitions are relatively weak (they represent only 1–2% of the total photon intensity), it was essential to maximize the detector solid angle. The construction of the Ortec photon spectrometer was such that it was not possible to place the source any closer than approximately 3 cm from the active volume of this detector, making the solid angle prohibitively small. The ^{126}Sn source was therefore mounted in an evacuated chamber, 1 cm from the front face of a Kevex Si(Li) detector 3 mm deep. The Si(Li) detector was cooled to liquid nitrogen temperature, and the input to the detector preamplifier was by way of a cooled field-effect transistor. The Si(Li) detector was shielded from β particles by means of a 0.010-cm Al foil absorber. The other detector, a 2.54-cm $\times$ 4.45-cm diam NaI(Tl) scintillator placed outside the chamber about 2 cm from the source, viewed the source through a 0.030-in. Al window.

The (21.7-42.6)-keV delayed-coincidence measurement was then undertaken, again using a fast-slow coincidence circuit with the Ortec TAC in the fast part. The TAC was started with photons detected in the Si(Li) detector and stopped with photons detected in the NaI(Tl) detector. In the slow part of the coincidence circuit, the two single-channel analyzers were set, respectively, to bracket the 21.7-keV peak of the Si(Li) spectrum and the 40–50-keV region of the NaI(Tl) spectrum.

There was reason to believe that the 21.7- and 42.6-keV γ rays are of dipole character. Therefore, in view of the lifetime systematics of 20- to 50-keV $M1$ and $E1$ transitions, the intermediate-state lifetime was expected to lie in the range from 1 to 100 ns. Consequently, every effort was made to minimize time jitter in both channels. In the "start" side [Si(Li) detector] the timing signal was taken directly from the preamplifier and was sent through a timing-filter amplifier to maximize the signal-to-noise ratio of the timing pulse viewed by the subsequent circuitry. The output of the timing-filter amplifier was sent through a Canberra extrapolated-zero-strobe discriminator (EZSD), and the fast timing pulse from the strobe was used as the input to the start channel of the TAC. The discriminator threshold of the EZSD was adjusted to be at a pulse height corresponding to 18-keV photons. On the stop side [NaI(Tl) detector] the fast pulse from the anode of the photo-

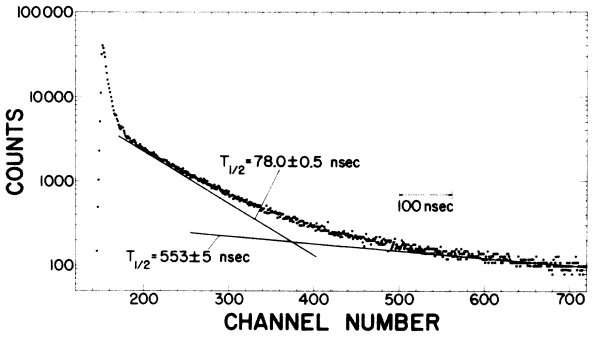

FIG. 2. Time spectrum from the time-to-amplitude-converter (TAC) obtained when β particles of energy $\leq$250 keV (detected in a plastic scintillator were used to generate start pulses and 64.3-, 86.9-, and 87.6-keV photons (detected in a NaI crystal) were used to produce stop pulses. The time distribution shows two half-life components, 78 and 553 ns, which are the half-lives of the 128.0- and 104.7-keV states, respectively (see Fig. 6).

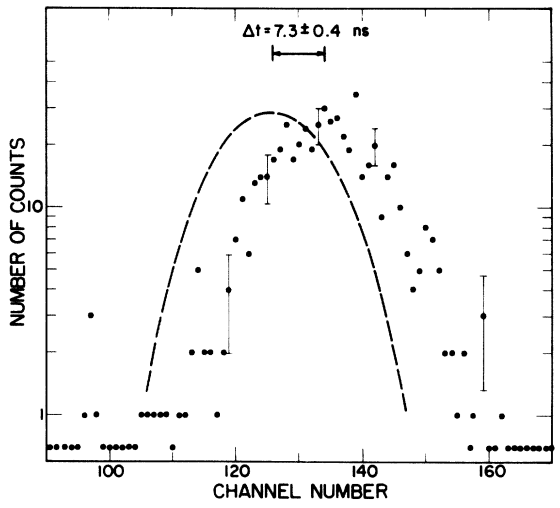

FIG. 3. Time spectrum from the TAC obtained when the start pulses were generated with 21.6-keV photons [detected in the cooled Si(Li) detector] and the stop pulses were produced with 42.6-keV photons (detected in the NaI crystal). The solid dots are the data obtained with the ^{126}Sn source. The dashed curve indicates the shape and position of the prompt time distribution, determined using a ^{165}Dy source (see text, Sec. II D).

multiplier tube was sent through a timing-filter amplifier and then through a fast discriminator into the "stop" channel of the TAC.

A prompt time spectrum was recorded with the above apparatus. The source used was ^{165}Dy, which decays to levels in ^{165}Ho. Fifteen percent of the ^{165}Dy β decays go to the 95-keV first excited state of ^{165}Ho, which decays by $M1$-$E2$ radiation to the ground state. Most of the remaining β transitions go to the ground state of ^{165}Ho. The half-life of the 95-keV state in ^{165}Ho is 0.022 ns.[9] The prompt time spectrum was measured under the same gating conditions as described above. The start channel was triggered with β particles in a narrow energy range bracketing 21 keV (the 0.010-cm Al absorber was removed) and the stop channel viewed the 40–50-keV energy region, which includes the 46.70- and 47.55-keV $K\alpha$ x rays of holmium. The time resolution of the system (FWHM of the prompt TAC spectrum) was thus determined to be approximately 15 ns.

The ^{165}Dy source was then removed and the ^{126}Sn source was placed in position and counted for one week. The resulting TAC spectrum is shown in Fig. 3, along with the observed shape and position of the prompt time distribution. The shapes of the prompt and delayed TAC spectra were observed to be quite similar, necessitating a centroid-shift analysis of the data. The ^{126}Sn TAC spectrum showed a shift to the right of the prompt time distribution (corresponding to a delay of the 42.6-keV γ ray relative to the 21.7-keV γ ray) of 7.3 ± 0.4 ns. This corresponds to an intermediate-state half-life of 5.1 ± 0.3 ns. In order to verify that there had been no time drifts during the long counting period, a second prompt spectrum was recorded after the ^{126}Sn run. It was determined that the shift of the prompt distribution during the ^{126}Sn counting period was at least an order of magnitude less than the statistical uncertainty in the centroid measurement.

E. Conversion-electron and γ-e^- coincidence measurements

The 3-mm Si(Li) detector, situated in the evacuated counting chamber, was used to record the electron spectrum emitted in the decay of ^{126}Sn. This spectrum is shown in Fig. 4. The intensities of the principal conversion lines are given in Table II. In deducing these intensities, we have assumed the same electron detection efficiency at all energies.

One of the noteworthy features of the spectrum of Fig. 4 is the relatively small peak to the left of the $L23.3$-$L22.7$ complex peak, which was not resolved in the previous measurements.[6] As discussed in Sec. III, we have concluded that this peak is mainly the L-conversion "line" of the previously unobserved isomeric transition from the 19-min first-excited state to the ground state of ^{126}Sb. In support of this conclusion, we were able to confirm, by means of a γ-e^- delayed coincidence measurement, that the transition in question is very delayed. In this experiment, the electron lines [observed with the 3-mm Si(Li) detector]

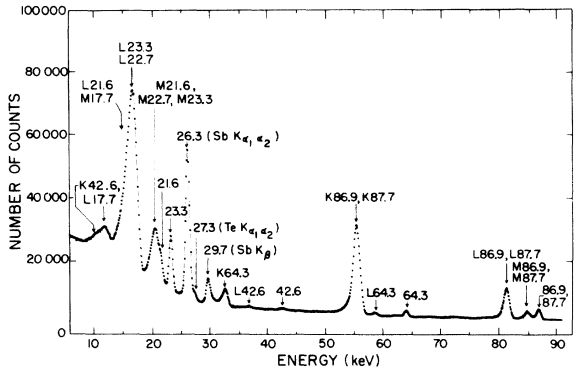

FIG. 4. The conversion-electron spectrum of ^{126}Sn measured with a 3-mm- thick by 80-mm^2 cooled Si(Li) detector. The conversion peaks are labeled with their associated transition energy and electron shell vacancy. Sb and Te x rays and γ rays were also detected and are labeled with their energies.

that are in coincidence with any photon [observed with the 2.54-×4.45-cm NaI(Tl) detector] were recorded in a multichannel analyzer. The coincidence resolving time for this measurement was 5 μs. In the resulting e^- coincidence spectrum, the peak in question was not present, indicating that it is delayed by >5 μs. Based on our interpretation of this peak as the L-conversion "line" of the $E3$ isomeric transition depopulating the 19-min state of ^{126}Sb, the energy of the isomeric state is 17.72 ± 0.030 keV.

In an attempt to prove independently that the e^- line of about 13 keV is associated with the 19-min isomer, samples of ^{126}Sb (19 min) were prepared and studied with the 3-mm Si(Li) spectrometer. The ^{126}Sb samples were electroplated onto copper foil from an acid solution containing ≈ 500 dis/s of ^{126}Sn. Unfortunately, this experiment was inconclusive because of the low over-all counting rate and the competing β background.

Several experiments were performed to establish the lifetime of the ^{126}Sb second excited state, which occurs at 40.4 keV (see Sec. III A). This state is strongly populated by the 87.6- and 64.3-keV transitions and is depopulated by the 22.7-keV transition. From analysis of the TAC spectrum recorded in a delayed-coincidence γ-e^- experiment, we concluded the lifetime of the 40.4-keV level is >100 μs. This result, in conjunction with other considerations, points to a multipolarity of $M2$ for the 22.7-keV transition. In view of the

TABLE II. Conversion-electron data for transitions in ^{126}Sb.

Electron line	Calculated intensity/100 β [a]		Observed relative intensity [b]
K42.6	3.2	13.9	3.3
L17.7	10.7 [c]		10.7
L21.6	2.1		
$(M+N)$17.7	3.3 [c]		
L22.7	57.9	94.9 + (<13.5)	90
L23.3	$M1$ 31.6		
	$E2$ < 13.5		
$(M+N)$21.6	0.54		
$(M+N)$22.7	16.1		
$(M+N)$23.3	$M1$ 8.1	27.3 + (<3.6)	24
	$E2$ < 3.6		
Sb K-LL Auger	≈2.6		
K64.3	5.4		5.4
L42.6	0.41		0.29
K86.9	16.4	25.1	28
K87.6	8.7		
L64.3	0.71		0.66
L86.9	6.3	7.4	8.5
L87.6	1.1		
$(M+N)$86.9	1.70	2.0	2.1
$(M+N)$87.6	0.29		

[a] Based on observed γ intensities (Table I), assigned multipolarities (Table III), and theoretical conversion coefficients (Ref. 17), except as noted. Uncertainties are typically ±10%.

[b] Normalized to the value in column 2 for the K64.3 line. Typical uncertainties in peak areas are ±15% for the stronger lines. Detector efficiency is assumed to be 100% at all energies.

[c] Based on requirement of intensity balance at the 17.7-keV level, assuming a 14% isomeric transition branch (see text).

116-s partial half-life[10] for the $M2$ transition that depopulates $^{124}Sb^{m1}$, we decided that the 40.4-keV state might have a half-life of several seconds, making it possible to observe the decay of this isomer directly, following a radiochemical separation. However, when freshly prepared ^{126}Sb sources, electroplated from a ^{126}Sn solution, were examined with a bare Si(Li) detector (*in vacuo*) and with a Be window gas proportional counter capable of detecting Sb L x rays, no evidence was found for a short-lived activity. These data suggest $T_{1/2}<10$ s. However, since the total activity of the ^{126}Sn in solution was only 500 dis/s and the electroplating efficiency was not well known, we do not place great reliance on this result.

Our final attempt to measure the half-life of the 40.4-keV state utilized the delayed-coincidence method of Glatz and Löbner.[11] This method involves a statistical analysis, with a PDP-8 computer, of the arrival times of all start and stop pulses from a TAC, and is capable of measuring half-lives up to 100 s. In our measurement, start pulses were taken from a NaI(Tl) detector (selected energy range: 30 keV $\lesssim E \lesssim$ 90 keV) and from a bare Si(Li) detector (25 keV $\lesssim E \lesssim$ 300 keV) in anticoincidence with pulses of E >90 keV from the NaI-(Tl) detector. The stop pulses were those of energy 14 keV $\lesssim E \lesssim$ 21 keV from the Si(Li) detector, in anticoincidence with pulses above noise from the NaI(Tl) detector. Data were recorded for about 18 days, using a portion ($\approx$ 50 dis/s) of the ^{126}Sn souce described in Sec. II A. Delayed coincidence counts in excess of the calculated accidental rate of $N_{acc} = 1.0996\times10^9$ per data point are shown in Fig. 5. A computer analysis of the gross data yielded $T_{1/2} = 11.1 \pm 10.5$ s. The large probable error results from the fact that "true" delayed coincidences amounted to only $\approx 2\times10^{-4}$ of the total coincidences. Assuming that the half-life is indeed 11 s, and using the known source strength and reasonable estimates of the start and stop pulse rates that arise from transitions which, respectively, populate and depopulate the 40.4 keV level, we calculate that in the first 2.4-s counting interval, the number of "true" delayed coincidences should have been $\approx 3.4\times10^5$. This number compares favorably with the observed value of 3.1×10^5 (*cf.* Fig. 5), again suggesting that the half-life is $\approx$ 11 s.

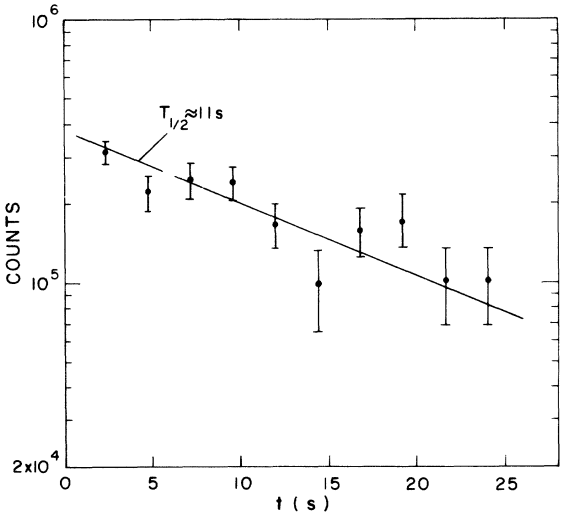

FIG. 5. Half-life measurement of the 40.4-keV level in ^{126}Sb. Each point represents the sum of the counts in 100 channels (2.4 sec), less 1.0996×10^9 accidental coincidences per point. The measuring time was 18 days.

III. DISCUSSION OF RESULTS

A. Decay scheme

A level scheme that summarizes the conclusions discussed in the following paragraphs is shown in Fig. 6. This scheme has the same basic structure as that proposed in Ref. 6, except that the energies of the transitions depopulating the first two excited states are now known, the order of the (21.6-42.6)-keV cascade has been determined, and the newly observed 86.9-keV transition has been placed in the scheme. The layout of this scheme is largely determined by the delayed coincidence results. However, in view of the high precision with which the γ-ray energy measurements were made and the relatively small number of γ rays in the ^{126}Sn spectrum, considerable weight could be place on energy balance considerations in verifying the placement

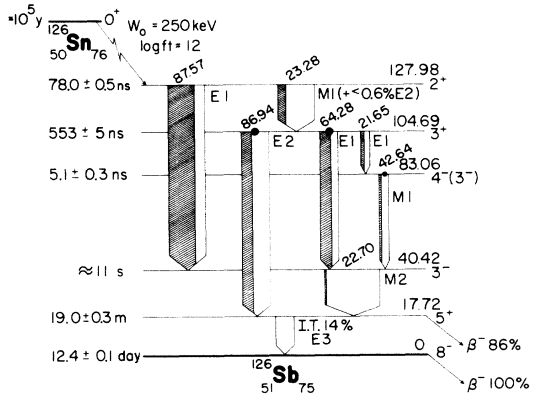

FIG. 6. The level scheme of ^{126}Sb. The widths of the arrows in the decay scheme indicate the *transition* intensity. The shaded portion of each arrow indicates the fraction of the transition intensity due to photons, and the remaining (unshaded) part represents the internal-conversion contribution.

of the various transitions. The achievement of an over-all intensity balance was, of course, another important guide. Finally, the proposed scheme is consistent with the deduced γ-ray multipolarity assignments discussed in succeeding sections.

Briefly, the arguments that lead to the proposed scheme are as follows. The 86.9-, 64.3-, and 42.6-keV transitions are known to follow the 553-ns half-life, as must also the 21.6-keV transition in view of the short (21.6-42.6)-keV delay ($T_{1/2}$ = 5.1 ns). Energy balance strongly suggests that the 64.28-keV transition parallels the (21.64-42.64)-keV cascade and that the 22.70-keV transition is in cascade with the 64.28-keV transition across the 86.94-keV gap. Since the 22.7-keV transition is more delayed ($T_{1/2} > 100$ μs) than the 64.3-keV transition, it must follow the 64.3-keV transition. Thus, these five transitions fix levels at 21.64, 64.28, and 86.94 keV *below* the 553-ns state. Next, the delayed coincidence measurements indicate that the strong 87.6- and 23.3-keV transitions depopulate a 78-ns state and that the 23.3-keV radiation *populates* the 553-ns state. From the fact that the energy sums (87.57 + 22.70) and (86.94 + 23.28) balance within the experimental uncertainties, and the 87.6-keV transition is not observed in coincidence with any γ ray, we conclude that the 87.6-keV transition immediately precedes the 22.7-keV transition. Finally, using our value of 17.72 keV for the energy of the $E3$ transition depopulating the 19-min isomer, we obtain for the energies of the excited states populated in the ^{126}Sn decay: 17.72, 40.42, 83.06, 104.69, and 127.98 keV.

B. Discussion of individual states of ^{126}Sb

1. 12.4-day, 19-min, and 0.55-μs states

In the work of Ref. 6 it was determined that the first excited state of ^{126}Sb has a half-life of 19.0 $\pm$ 0.3 min and decays 86% by β decay to levels in ^{126}Te and 14% by an isomeric transition to the ground state of ^{126}Sb. The possible spin and parity assignments are limited to $(5, 6, 7)^+$ on the basis of the allowed β decay (logft = 5.9) of this state to the 1774-keV 6^+ level in ^{126}Te.[6] However, it was noted in Ref. 6 that from shell-model considerations the 19-min state could only be assigned spin and parity 5^+, since this is the highest spin possible for a positive parity state with the available neutron ($h_{11/2}$, $d_{3/2}$, and $s_{1/2}$) and proton ($g_{7/2}$, $d_{5/2}$) shell-model orbitals.

The partial lifetime of the 17.7-keV isomeric transition is 8.1×10^3 s. Based upon theoretical transition probabilities[12] and the systematics of the lifetimes of electromagnetic transitions,[13] the multipolarity of this isomeric transition can only be $E3$, which fixes the ground-state spin and parity of ^{126}Sb as 8^-. (The 2^- possibility can be excluded because such a state would be strongly populated in the ^{126}Sn β decay.) The 8^- assignment for the 12.4-day state is independently supported by the observed β decay of this state to the $6^+, 8^+, 10^+$, and (9^-) levels of ^{126}Te.[14] In addition, the magnetic moment of the ^{126}Sb ground state has been measured by Krane and Steyert.[15] *Assuming* $I = 8$, they obtain $|\mu| = (1.28 \pm 0.07)$ μ_N, which is consistent with the theoretical estimate[16] of + 1.26 μ_N for a $[\pi(g_{7/2})^1 \nu(h_{11/2})^{11}]^{8^-}$ configuration. However, as pointed out in Ref. 15, the deduced value of μ is rather insensitive to the assumed value of I and does not provide a conclusive independent check of the 8^- assignment.

2. 40.4-keV state

Our data indicate that the half-life of the 40.4-keV second excited state is $\approx$11 s. Consideration of γ-ray lifetime systematics[13] leads to the conclusion that the 22.7-keV depopulating transition is mainly of multipolarity $M2$, with very little $E3$ admixture. From the total conversion coefficient of the 22.7-keV transition, one can obtain additional multipolarity information. Based on the γ-intensity data of Table I and assuming that the three transitions (87.57, 64.28, and 42.64 keV) feeding the 40.4-keV level are pure dipole transitions, one obtains α_{total} (22.7 keV) $\approx$ 670. The theoretical[17] total internal conversion coefficient for a 22.7-keV $M2$ transition is 741, whereas that for an $E3$ transition is 7.3×10^4, again indicating that the transition is predominantly $M2$.

The $M2$ character of the 22.7-keV transition requires the spin and parity of the 40.42-keV level to be 3^- or 7^-. The absence of a crossover transition to the 8^- ground state, coupled with the observed strong population of this state from low-spin states higher in the scheme (*cf.* following sections), leaves no doubt but that 3^- is the proper choice.

3. Levels at 128.0 and 104.7 keV

The previous conclusion[6] that the ^{126}Sn 0^+ ground state decays predominantly to the level depopulated by the 87.6- and 23.3-keV transitions is supported by the present work. The β end-point energy[6] of 250 $\pm$ 30 keV and the ^{126}Sn ground-state half-life[6] of $\approx 10^5$ yr yields log$ft \approx 12$ for this β transition. This β decay is therefore almost certainly second forbidden, and so the only possible spin and parity assignments for the 128.0-keV level are $(2, 3)^+$, with 2^+ being favored by logft systematics.[18]

The 87.6-keV γ ray connects this positive-parity

level with the 40.4-keV negative-parity level. The only parity-changing multipolarity consistent with the lifetime of this transition is $E1$. This means that the spin of the 40.4-keV state must lie between 1 and 4. β feeding considerations rule out spins 1 and 2, and spin 4 is eliminated by the $M2$ multipolarity of the 22.7-keV transition, again leaving only the 3^- choice (see previous section).

The 104.7-keV level depopulates to the 3^- level via the 64.3-keV transition. Based on the relative strength of the 64.3-keV γ ray and the 64.3 K line in the spectrum of Fig. 4, with appropriate correction for the γ-ray efficiency of the 3-mm Si(Li) detector, we calculate $\alpha_K(64.3) \approx 0.5$, which establishes the multipolarity of this transition as $E1$ [at 64.3 keV, the two lowest theoretical[17] α_K values are $a_K(E1) = 0.56$ and $\alpha_K(M1) = 1.91$]. Thus, the possible assignments for the 104.7-keV level are restricted to $(2, 3, 4)^+$. We next consider the 86.9-keV transition, which proceeds to the 5^+ state. The observed K/L ratio for the (86.9, 87.6)-keV doublet is 3.31 ± 0.50. Since the 87.6-keV transition is an $E1$, for which the theoretical[17] K/L value is 7.74, one immediately suspects that the 86.9-keV transition is $E2$. [Note: for this energy, $(K/L)_{M1} = 7.8$, $(K/L)_{E2} = 2.6$.] In fact, calculation of the doublet K/L ratio on the basis of the observed 86.9- and 87.6-keV photon intensities and the theoretical conversion coefficients, assuming the 86.9-keV transition to be $E2$, yields $(K/L)_{\text{doublet}} = 3.38$. We therefore conclude that the 86.9-keV transition is pure $E2$, which establishes the spin and parity of the 104.7-keV level as 3^+.

The assigned spins of the 128.0- and 104.7-keV levels require the character of the 23.3-keV connecting transition to be $M1(+E2)$. If one assumes that β feeding of the 104.7-keV state is negligible, an upper limit on the amount of $E2$ admixture in the 23.3-keV transition can be calculated on the basis of intensity balance at the 553-ns level. [Note: at 23.3 keV, $\alpha_{\text{total}}(M1) = 6.21$, $\alpha_{\text{total}}(E2) = 475$.[17]] Using pure multipolarities for the 86.9-keV ($E2$), 21.6-keV ($E1$) (see next section), and 64.3-keV ($E1$) transitions, we obtain a total intensity *out* of the 104.7-keV level of 144 ± 15 units, normalized to the intensity scale of Table I. If the 23.3-keV transition is assumed to be pure $M1$, its total intensity calculates to be 125 ± 12. The total intensity of the $E2$ component must therefore lie somewhere between zero and 46 units, giving a limit on the $E2/M1$ mixing ratio of $\delta^2 < 0.0056$.

The present data do not exclude the possibility that there is a weak β branch to the 104.7-keV 3^+ level. It is evident from the arguments presented in the preceding paragraph that the intensity of this β transition must be ≤ 46 units (or $\leq 15\%$), yielding a limit on the logft value of ≥ 12.9, which is the approximate lower limit of known logft values for $\Delta I = 3$, $\Delta\pi = 0$ transitions.[18]

4. *Level at 83.1 keV*

The 83.1-keV level is populated solely by a 21.6-keV transition, and is depopulated by a 42.6-keV transition. Since these transitions are in cascade between 3^+ and 3^- states, they cannot be of the same multipolarity. The requirement of intensity balance results in a simple relationship between their total internal conversion coefficients. This relationship is shown in Fig. 7, where the uncertainty in the photon intensity measurements has been taken into account. It is clear from this figure that the 42.7-keV γ ray cannot be $E1$. In fact, the only consistent multipolarity assignments for the 21.6- and 42.6-keV γ rays are $E1$ and $M1(+E2)$, respectively. Higher-order multipolarity assignments for these two γ rays (with the same parity relationship) are ruled out by the 5.1-ns lifetime of the 83.1-keV level.

The above multipolarities for the 21.6- and 42.6-keV γ rays limit the possible spin and parity assignments for the 83.1-keV state to $(2, 3, 4)^-$. The

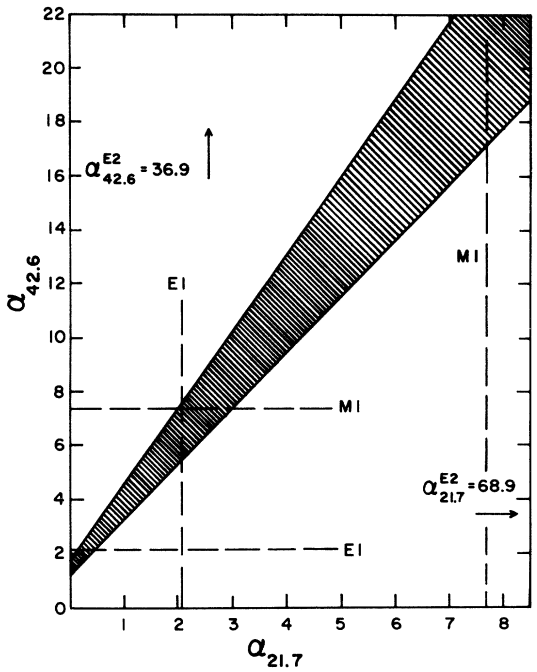

FIG. 7. The relationship between the total internal-conversion coefficients of the 42.6- and 21.7-keV transitions, which is determined by the intensity balance requirement at the 83.1-keV level (see text, Sec. III B 3). The shaded region represents the uncertainty in this linear relationship resulting from the experimental uncertainties in the measured photon intensities.

2^- possibility can be immediately ruled out since in this case there would be strong β decay to the level. The 3^- possibility is also very unlikely, since, in this case, one would expect the level to be populated strongly by an $E1$ transition from the 2^+ level. The data thus strongly favor a 4^- assignment. The apparent absence of the 65.34-keV ($4^- \rightarrow 5^+$) $E1$ transition is understandable: a reasonable estimate for the hindrance factor of this transition is $F_W \approx 10^6$ (*cf.* Table III), which implies only $\approx 1\%$ branching to the 5^+ level.

C. Summary of e^-, multipolarity, and transition-probability data

The deduced multipolarity assignments are summarized in Table III. Except for the 23.3-keV transition, which possibly has a small $E2$ component, lifetime considerations suggest that all of the other transitions are essentially pure multipoles. Based on these multipolarity assignments, the photon intensity data from Table I, and the theoretical conversion coefficients,[17] one can calculate the expected conversion-electron line intensities. As shown in Table II, the extent of agreement between these calculations and the observed electron-line intensities is reasonably good, giving added support both to the proposed assignments and to the over-all decay scheme. There is a tendency for the intensity ratios $I_{e^-}(\text{exp.})/I_{e^-}(\text{calc.})$ to drop somewhat as the energy decreases--an effect attributable to the increasing importance of electron absorption and straggling phenomena at the lower energies. No correction has been made for this effect.

The above data, in combination with the observed lifetimes of the levels in ^{126}Sb, yield the Weisskopf hindrance factors, $F_W = T_{1/2\gamma}(\text{exp})/T_{1/2\gamma}$ (Weissk.), given in Table III. All of the F_W values lie within the empirical ranges[13] for the specified multipolarities.[19]

IV. MODEL CONSIDERATIONS AND ENERGY LEVEL SYSTEMATICS

A. Shell-model assignments

To provide a basis for a tentative theoretical interpretation of the observed ^{126}Sb levels, we first consider the single-particle shell-model orbitals available to the odd proton and odd neutron. The level systematics of the odd-A antimony ($Z = 51$) isotopes[21-23] indicate that, at neutron number $N = 75$, the $g_{7/2}$ proton quasiparticle state is lowest lying, with the $d_{5/2}$ state a few hundred keV higher in energy. Since the $d_{3/2}$, $s_{1/2}$, and $h_{11/2}$ levels are considerably higher in energy than the $d_{5/2}$ level, their contribution to the proton configurations of the low-lying states of ^{126}Sb is expected to be negligible. Studies of the odd-neutron nuclei near ^{126}Sb indicate that the $h_{11/2}$, $d_{3/2}$, and $s_{1/2}$ quasiparticle states are within 100 keV of the ground state and that the $d_{5/2}$ and $g_{7/2}$ states lie several hundred keV below the neutron Fermi level.

The odd-odd shell-model states that can be formed by coupling the above proton ($g_{7/2}$, $d_{5/2}$) and neutron ($d_{3/2}$, $s_{1/2}$, $h_{11/2}$) configurations have I^π values that range from 1^+ to 5^+ and from 2^- to 9^-. The components that we would expect to contribute the bulk of the single-particle character of the observed low-lying states of ^{126}Sb are listed in Table IV. On the basis of odd-Z energy systematics and magnetic-moment data,[24] it seems probable that the components involving $\pi g_{7/2}$ have much larger amplitudes than those involving $\pi d_{5/2}$. Collective components, although undoubtedly present, are expected to play a relatively

TABLE III. Experimental half-lives and hindrance factors for γ-ray transitions in ^{126}Sb.

Transition energy (keV)	Assigned multipolarity	α total (theoretical) [a]	$I_\gamma/100\ \beta$	$I_T/100\ \beta$ [b]	$T_{1/2\gamma}$(exp.) (s)	$T_{1/2\gamma}$(Weissk.) (s)	F_W
17.7	$E3$	3.27×10^5	···	14.0 [c]	2.7×10^{9}	2.3×10^{6}	1.2×10^{3}
21.6	$E1$	2.15	1.24	3.9	2.4×10^{-5}	2.6×10^{-11}	9.1×10^{5}
22.7	$M2$	7.41×10^2	0.10	73.8	$\approx 8.1\times10^{3}$ [d]	1.8×10^{-1}	$\approx 4.5\times10^{4}$
23.3 [e]	$M1$ [e]	6.21	6.38	46.0	1.2×10^{-6}	1.8×10^{-9}	6.8×10^{2}
	$E2$ [e]	4.75×10^2	<0.036	<16.9	$>2.2\times10^{-4}$	2.2×10^{-3}	$>1.0\times10^{-1}$
42.6	$M1$	7.41	0.50	4.2	4.3×10^{-8}	2.9×10^{-10}	1.5×10^{2}
64.3	$E1$	0.656	9.54	15.8	3.1×10^{-6}	1.0×10^{-12}	3.1×10^{6}
86.9	$E2$	2.75	8.88	33.3	3.3×10^{-6}	3.0×10^{-6}	1.1
87.6	$E1$	0.276	36.8	47.0	2.1×10^{-7}	4.0×10^{-13}	5.2×10^{5}

[a] See Ref. 17.

[b] Using the normalization $I_T(87.6) + I_T(86.9) + I_T(64.3) + I_T(21.6) = 100$.

[c] Value consistent with both the $L17.7$ conversion-line intensity and the isomeric-transition branching ratio of Ref. 6.

[d] Based on a half-life of 11 s for the 40.4-keV level.

[e] $\delta^2(E2/M1) < 0.0056$ is assumed (see text).

minor role in the structure of these low-lying states.[3]

No theoretical level-spectra calculations have yet been made for ^{126}Sb. However, the calculations of True, Kisslinger, and Thankappan[3] for ^{124}Sb should give some insight as to what is "reasonable" at mass 126. In their calculations, they took into account the pairing interaction and a simplified form of the residual neutron-proton two-body interaction. Quasiparticle-phonon interactions, which are expected to be relatively unimportant in the odd-odd Sb nuclei, were neglected. They predict (in the ^{124}Sb case) a 5^+ ground state, with 2^+ and 3^+ being the next highest positive-parity states (at ≈ 50 keV), and with 4^+, 3^-, 4^-, 5^-, 6^-, 7^-, and 8^- all occurring between 80 and 120 keV. Although they caution that, because of the high density of states and the semiquantitative nature of their calculational methods, all they can hope to do is reproduce general trends in the data, the following comparisons are worth noting: (a) The six states we observe in ^{126}Sb are among those *predicted* to occur at very low energy; (b) the negative-parity levels lie somewhat lower in energy (relative to the positive-parity levels) than the calculations suggest; and (c) the energy spread of the negative-parity levels is larger than predicted. Obviously, (b) and (c) may be related.

It is interesting to consider the transition probabilities of certain electromagnetic transitions in ^{126}Sb in the light of the single-particle context presented above. The $E3$ transition from the 17.7-keV 5^+ state to the 8^- ground state cannot proceed via the components listed in Table IV and it must therefore involve other single-particle components, the amplitudes of which are expected to be very small. Thus, the relatively large Weisskopf hindrance factor of 1.2×10^3 for this transition is understandable. The analogous $E3$ transition in ^{128}Sb (assuming $E_\gamma = 15$ keV) is $F_W \approx 2\times10^3$, and the one in ^{124}Sb($8^- \rightarrow 5^+$) has $F_W \approx 2.6\times10^2$.

TABLE IV. Two-quasiparticle components expected to contribute to the structure of the observed low-lying states of ^{126}Sb.

I^π [energy (keV)]	Probable major components	Possible admixed components
2^+ (127.9)	$(\pi 1g_{7/2}\nu 2d_{3/2})$	$(\pi 2d_{5/2}\nu 2d_{3/2})$
		$(\pi 2d_{5/2}\nu 3s_{1/2})$
3^+ (104.7)	$(\pi 1g_{7/2}\nu 2d_{3/2})$	$(\pi d_{5/2}\nu 2d_{3/2})$
	$(\pi 1g_{7/2}\nu 3s_{1/2})$	$(\pi 2d_{5/2}\nu 3s_{1/2})$
4^- (83.1)	$(\pi 1g_{7/2}\nu 1h_{11/2})$	$(\pi 2d_{5/2}\nu 1h_{11/2})$
3^- (40.4)	$(\pi 1g_{7/2}\nu 1h_{11/2})$	$(\pi 2d_{5/2}\nu h_{11/2})$
5^+ (17.7)	$(\pi 1g_{7/2}\nu 2d_{3/2})$	...
8^- (0.0)	$(\pi 1g_{7/2}\nu 1h_{11/2})$	$(\pi 2d_{5/2}\nu 1h_{11/2})$

The $M2$ transition from the 40.4-keV 3^- level to the 17.7-keV 5^+ level is also of interest from the single-particle standpoint. Here again the transition cannot proceed via the suggested main components in the two wave functions. The approximately 11-sec half-life of this transition yields $F_W \approx 4.5\times10^4$. The analogous $M2$ transition ($5^+ \rightarrow 3^-$) in ^{124}Sb has $F_W \approx 4\times10^5$, a value considerably larger than that of any other known $M2$ transition in spherical nuclei. This suggests, e.g., that the amplitude of $|\pi g_{7/2}, \nu g_{7/2}\rangle$ in the ^{124}Sb 5^+ state is exceedingly small.

The transition probability of the 86.9-keV $E2$ transition is about one single-particle unit. This transition is much faster than the analogous 75-keV ($5^+ \rightarrow 3^+$) $E2$ transition in ^{122}Sb, for which $F_W \approx 420$. On the other hand, it is considerably slower than some of the low-energy $E2$ transitions observed in nearby odd-neutron nuclei (see, e.g., Refs. 25 and 26). It would thus appear that the collective contribution to the 86.9-keV transition is small, but not negligible. The full significance of this transition rate will not be apparent until detailed model calculations are available for comparison.

B. Level systematics of the odd-odd antimony nuclei

We show in Fig. 8 the low-lying levels and other pertinent data for ^{120}Sb (Refs. 16, 24, 27, and 28), ^{122}Sb (Refs. 16, 29–31), ^{124}Sb (Refs 10, 16 and 31), ^{126}Sb (Ref. 32 and present work), ^{128}Sb. (Refs. 15, 24, and 33), and ^{130}Sb (Refs. 5 and 34). The results reported here for ^{126}Sb yield the most complete set of low-lying level spins, parities and lifetimes of all of the odd-odd antimony nuclei.

It is interesting to note that, in agreement with theoretical expectations,[3,5] there are no 9^- states [which would result from the aligned coupling of the $(\pi g_{7/2}, \nu h_{11/2})$ configuration] observed among the lowest lying levels of these nuclei. The 8^- state, however, occurs rather low in excitation in all cases and becomes the ground state in ^{126,128}Sb and possibly also in ^{130}Sb.

The drop in the 5^+ level [presumably $(\pi g_{7/2}, \nu d_{3/2})$] and the obvious rise in the 1^+ level [presumably $(\pi d_{5/2}, \nu d_{3/2})$] beyond ^{120}Sb is undoubtedly related to the fact that in the odd-A Sb nuclei, $d_{5/2}$ is the ground state for $N \leq 70$, while for $N > 70$ $g_{7/2}$ occurs as the ground state, with $d_{5/2}$ rising rapidly in energy as a function of increasing N (*cf.* Fig. 8, Ref. 21). As mentioned above, the

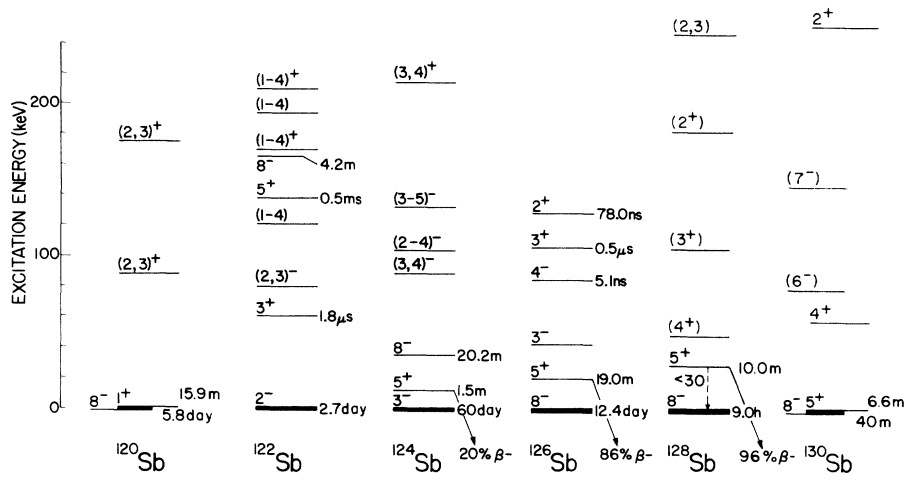

FIG. 8. The low-lying energy level systematics of the odd-odd antimony isotopes with neutron numbers $N = 71-79$. In ^{120}Sb and ^{130}Sb the relative position of the isomers is unknown; thus, both are plotted at $E = 0$. In ^{120,128,130}Sb, states of the same parity are plotted relative to each other.

occurrence of 5^+ as the lowest-lying positive-parity state in ^{124}Sb is in agreement with the prediction of True *et al.*,[3] and for this state to persist as the lowest positive-parity state in ^{126}Sb and probably also in ^{128,130}Sb seems entirely reasonable.

It is clear that the odd-odd Sb isotopes offer theorists a valuable opportunity to learn more about the residual nuclear forces, but a consistent interpretation of the level structure of these nuclei will undoubtedly require more complete data (particularly I^π assignments) than are now available. Through present techniques, notably high-resolution charged-particle reaction spectroscopy and (n,γ) spectroscopy, it can be hoped that our knowledge of these nuclei will be expanded considerably in the near future.

ACKNOWLEDGMENTS

The authors would like to thank Dr. J. J. Malanify and Dr. C. J. Umbarger of this laboratory for making the Si(Li) photon spectrometer available for our use. We also extend our thanks to Dr. H. W. Jones for his assistance with some of the measurements. One of the authors (K.E.G.L.) gratefully acknowledges a fellowship from the German Bundesministerium für Bildung und Wissenschaft, and he also would like to express appreciation for the hospitality shown him at the Los Alamos Scientific Laboratory.

---

† Work supported by the U. S. Energy Research and Development Administration.

*Present address: Department of Physics, Indiana University, Bloomington, Indiana 47401.

[1]M. H. Brennan and A. M. Bernstein, Phys. Rev. 120, 927 (1960).

[2]L. S. Kisslinger and D. M. Rote, Phys. Rev. Lett. 16, 659 (1966).

[3]W. W. True, L. S. Kisslinger, and V. K. Thankappan, University of California at Davis, Crocker Nuclear Laboratory Report No. UCD-CNL-87, 1966 (unpublished).

[4]D. M. Rote, Ph.D. thesis, Western Reserve University, Cleveland, Ohio, 1967 (unpublished; available from University Microfilms, No. 67-8849).

[5]A. Kerek, P. Carlé, and S. Borg. Nucl. Phys. A224, 367 (1974).

[6]C. J. Orth, B. J. Dropesky, and N. J. Freeman, Phys. Rev. C 3, 2402 (1971).

[7]N. J. Freeman *et al.*, in *Electromagnetic Separation of Radioactive Isotopes*, edited by M. J. Higatsberger and F. P. Wiehbock (Springer-Verlag, Berlin, Germany, 1961), pp. 83–102.

[8]C. F. Perdrisat, Rev. Mod. Phys. 38, 41 (1966).

[9]A. Buyrn, Nucl. Data B11, 189 (1974).

[10]F. E. Bertrand, Nucl. Data B10, 91 (1973).

[11]J. Glatz and K. E. G. Löbner, Nucl. Instrum. Methods 94, 237 (1971).

[12]S. A. Moszkowski, Phys. Rev. 89, 474 (1953).

[13]M. Goldhaber and A. W. Sunyar, in *Alpha-, Beta- and Gamma-Ray Spectroscopy*, edited by K. Siegbahn, (North-Holland, Amsterdam, 1966).

[14]M. E. Bunker, J. W. Starner, and C. J. Orth, Bull Am. Phys. Soc. 18, 680 (1973).

[15]K. S. Krane and W. A. Steyert, Phys. Rev. C 6, 2268 (1972).

[16]P. T. Callaghan, M. Shott, and N. J. Stone, Nucl. Phys. A221, 1 (1974).
[17]R. S. Hager and E. C. Seltzer, Nucl. Data A4, 1 (1968).
[18]S. Raman and N. B. Gove, Phys. Rev. C 7, 1995 (1973).
[19]It should be noted that the hindrance factors compiled in Ref. 13 are determined using the single-particle transition probability estimates of Moszkowski (Ref. 12). The differences between these "Moszkowski hindrance factors" and Weisskopf hindrance factors are tabulated in Ref. 20.
[20]A. H. Wapstra, G. J. Nijgh, and R. Van Lieshout, *Nuclear Spectroscopy Tables* (North-Holland, Amsterdam, 1959), p. 71.
[21]E. U. Baranger, in *Advances in Nuclear Physics*, edited by M. Baranger and E. W. Vogt (Plenum, New York, 1971), Vol. 4, p. 261.
[22]G. Vanden Berghe and K. Heyde, Nucl. Phys. A163, 478 (1971).
[23]A. G. de Pinho, J. M. F. Jeronymo, and I. D. Goldman, Nucl. Phys. A116, 408 (1968).
[24]C. Ekström, W. Hogervorst, S. Ingelman, and G. Wannberg, Nucl. Phys. A226, 219 (1974).
[25]R. A. Sorensen, Phys. Rev. 133, B281 (1964).
[26]M. Schmorak, A. C. Li, and A. Schwarzschild, Phys. Rev. 130, 727 (1963).
[27]S. A. Hjorth, Ark. Fysik 33, 183 (1967).
[28]A. D. Jackson, Jr., E. H. Rogers, Jr., and G. J. Barrett, Phys. Rev. 175, 65 (1968).
[29]F. E. Bertrand, Nucl. Data B7, 419 (1972).
[30]P. Heubes, H. Ingwersen, W. Klinger, W. Lampert, W. Loeffler, G. Schatz, and W. Witthuhn, Phys. Rev. C 7, 2128 (1973).
[31]E. B. Shera (private communication).
[32]R. L. Auble, Nucl. Data B9, 125 (1973).
[33]N. Imanishi, I. Fujiwara, and T. Nishi, Nucl. Phys. A238, 325 (1975).
[34]H. R. Hiddleston and C. P. Browne, Nucl. Data B13, 133 (1974).